Prey-Predator Model with a Nonlocal Bistable Dynamics of Prey

Malay Banerjee [1],*,[†], Nayana Mukherjee [1],[†] and Vitaly Volpert [2],[†]

1   Department of Mathematics and Statistics, IIT Kanpur, Kanpur 208016, India
2   Institut Camille Jordan, UMR 5208 CNRS, University Lyon 1, 69622 Villeurbanne, France;
    volpert@math.univ-lyon1.fr
*   Correspondence: malayb@iitk.ac.in; Tel.: +91-0512-259-6157
†   These authors contributed equally to this work.

Abstract: Spatiotemporal pattern formation in integro-differential equation models of interacting populations is an active area of research, which has emerged through the introduction of nonlocal intra- and inter-specific interactions. Stationary patterns are reported for nonlocal interactions in prey and predator populations for models with prey-dependent functional response, specialist predator and linear intrinsic death rate for predator species. The primary goal of our present work is to consider nonlocal consumption of resources in a spatiotemporal prey-predator model with bistable reaction kinetics for prey growth in the absence of predators. We derive the conditions of the Turing and of the spatial Hopf bifurcation around the coexisting homogeneous steady-state and verify the analytical results through extensive numerical simulations. Bifurcations of spatial patterns are also explored numerically.

Keywords: prey-predator; nonlocal consumption; Turing bifurcation; spatial Hopf bifurcation; spatio-temporal pattern

1. Introduction

Investigation of spatiotemporal pattern formation leads to understanding of the interesting and complex dynamics of prey-predator populations. Reaction-diffusion systems of equations are conventionally used to study such dynamics. Various forms of reaction kinetics in the spatiotemporal model give rise to a wide variety of Turing patterns as well as non-Turing patterns including traveling wave [1–5] and spatiotemporal chaos [6,7]. Such patterns can be justified ecologically with the help of the field data and experiments which confirm the presence of patches in the prey-predator distributions. For example, Gause [8] has shown the importance of spatial heterogeneity for the stabilization and long term survival of species in the laboratory experiment on growth of *paramecium* and *didinium*. Luckinbill [9,10] has also studied the effect of dispersal on stability as well as persistence/extinction of population over a longer period of time. Based on these data, works are done where the prey-predator models with spatial distribution are considered for various ecological processes [11], such as plankton patchiness [12–14], semiarid vegetation patterns [15], invasion by exotic species [16,17] etc. (see also [18–21]). Such models have been successful in proving long term coexistence of both prey and predator populations along with formation of stationary or time dependent localized patches with periodic, quasi-periodic and chaotic dynamics [6,7].

The classical representation of two species interacting populations including the spatial aspect, consists of a reaction-diffusion system of equations in the form of two nonlinear coupled partial differential equations,

$$\frac{\partial u}{\partial t} \;=\; d_u \frac{\partial^2 u}{\partial x^2} + F_1(u,v), \tag{1}$$

$$\frac{\partial v}{\partial t} \;=\; d_v \frac{\partial^2 v}{\partial x^2} + F_2(u,v) \tag{2}$$

with non-negative initial conditions and appropriate boundary conditions. Population densities of prey and predator species at the spatial location x and time t are denoted by $u(x,t)$ and $v(x,t)$, respectively. The nonlinear functions F_1 and F_2 represent the interactions among individuals of the two species. The diffusion coefficients d_u and d_v represent the rate of random movement of individuals of the two species within the considered domain.

A wide variety of spatiotemporal patterns are described by these models, namely, traveling wave, periodic traveling wave, modulated traveling wave, wave of invasion, spatiotemporal chaos, stationary patchy patterns etc. [20–23]. Among all these, only stationary patchy pattern results in due to Turing instability, represents a stationary in time but non-homogeneous in space distribution. A stable co-existence of both species occurs due to formation of localized patches where the average population of each species remains unaltered in time. Whereas the other patterns are time dependent with the individuals of both species following continuously changing resources.

The general assumption for consumption of resources in the spatiotemporal models of interacting populations is taken to be local in space. In other words, it is supposed that the individuals consume resources in some areas surrounding their average location. Whereas nonlocal consumption of resources is more general since it incorporates the interspecific competition for food [24–26]. Such modifications enables the explanation of emergence and evolution of biological species as well as speciation in a more appropriate manner [27–31]. The models with nonlocal consumption of resources present complex dynamics for the single species models [28,29,32–35] as well as for competition models including two or more species [32,36–38]. Furthermore, such complex dynamics cannot be found in the corresponding local models.

Interesting results are obtained due to the introduction of nonlocal consumption of prey by predator in a reaction-diffusion system with Rosenzweig-McArthur type reaction kinetics [39]. Contrary to the local model where Turing patterns are not observed, this model satisfies the Turing instability conditions and gives rise to Turing patterns under proper assumptions on parameters. Other than this, existence of non-Turing patterns like traveling wave, modulated traveling wave, oscillatory pattern and spatiotemporal chaos are also observed for the nonlocal model. Some of the non-Turing patterns are reported for the nonlocal model with the modified Lotka-Volterra reaction kinetics [39,40].

In order to introduce the prey-predator model with a nonlocal bistable dynamics of prey, let us recall the classical models for the single population. Single species population model with the logistic growth law is described by the following ordinary differential equation, assuming homogeneous distribution of the species over their habitat,

$$\frac{du}{dt} \;=\; ru(k-u), \tag{3}$$

where r and k denote the intrinsic growth rate and carrying capacity, respectively. Introducing multiplicative Allee effect in this single population growth model, the above equation becomes

$$\frac{du}{dt} \;=\; ru(k-u)(u-l), \tag{4}$$

where l is the Allee effect threshold satisfying the restriction $0 < l < k$ [41–45]. This equation accounts for two significant feedback effects: positive feedback due to cooperation at low population density and negative feedback arising through the competition for limited resources at high population density [46]. In the framework of this formulation, the cooperation and competition mechanisms are described by the linear factors $(u-l)$ and $(k-u)$, respectively. Introduction of the Allee effect through a multiplicative term has a significant drawback since it represents a product of cooperation at the

low population density and competition at the high population density. In this case, cooperation and competition influence each other, and their effects cannot be considered independently (see [46,47] for detailed discussion). The per capita growth rate is described by the factor $r(k-u)(u-l)$ which is positive for $l < u < k$, it is an increasing function for $l < u < \frac{k+l}{2}$, and a decreasing function for $\frac{k+l}{2} < u < k$. To overcome such situations, an additive form of the per capita growth rate function, proposed by Petrovskii et al. [47], is given by

$$\frac{du}{dt} = u\left(f(u) - \sigma - g(u)\right), \tag{5}$$

where the functions $f(u)$ and $g(u)$ describe population growth due to the reproduction and density dependent enhanced mortality rate, respectively. Here σ is the natural mortality rate independent of population density. Depending upon appropriate parametrization and assumption for the functional forms, the above model describes various types of single species population growth. In particular, if we choose $f(u) = \mu u$ and $g(u) = \eta u^2$ then we get the growth Equation (4) from (5) with appropriate relations between two sets of parameters (r, k, l) and (μ, σ, η). With a different type of parametrization, $f(u) = abu$ and $g(u) = au^2$ we can obtain the single species population growth model with sexual reproduction [34,35,48] as follows

$$\frac{du}{dt} = au^2(b-u) - \sigma u, \tag{6}$$

where a is the intrinsic growth rate, b is the environmental carrying capacity and σ is the density independent natural death rate. Introducing the nonlocal consumption of resources and random motion of the population, we get the following integro-differential equation model,

$$\frac{\partial u(x,t)}{\partial t} = d\frac{\partial^2 u(x,t)}{\partial x^2} + au^2(x,t)\left(b - \int_{-\infty}^{\infty} \phi(x-y)u(y,t)dt\right) - \sigma u(x,t), \tag{7}$$

where $\phi(z)$ is an even function with a bounded support and d is the diffusion coefficient. The kernel function is normalized to satisfy the condition $\int_{-\infty}^{\infty} \phi(z)dz = 1$. It shows the efficacy of consumption of resources as a function of distance $(x-y)$. The integral describes the total consumption of resources at the point x by the individuals located at $y \in (-\infty, \infty)$. This model shows bistability since the corresponding temporal model has two stable steady-states 0 and u_+ separated by an unstable steady-state u_- [34].

Based on this model, we are interested to study pattern formation described by the nonlocal reaction-diffusion system of prey-predator interaction with the bistable reaction kinetics of prey in the absence of predators which are specialist in nature following Holling type-II functional response. We will obtain the conditions of the Turing instability and of the spatial Hopf bifurcation in Section 2. Section 3 describes spatiotemporal pattern formation observed in numerical simulations. Here we also present bifurcation diagrams for the model with nonlocal consumption. Main outcomes of this investigation are summarized in the discussion section.

2. Stability Analysis

In this section, we will introduce the prey-predator models without and with nonlocal consumption term and will study stability of the positive homogeneous stationary solution.

2.1. Local Model

We consider the following reaction-diffusion system for the prey-predator interaction:

$$\frac{\partial u}{\partial t} = d_1\frac{\partial^2 u}{\partial x^2} + au^2(b-u) - \sigma_1 u - \frac{\alpha uv}{\kappa + u}, \tag{8}$$

$$\frac{\partial v}{\partial t} = d_2\frac{\partial^2 v}{\partial x^2} + \frac{\beta uv}{\kappa + u} - \sigma_2 v, \tag{9}$$

subjected to a non-negative initial condition and the periodic boundary condition. The consumption of prey by the predator follows the Holling type-II functional response, α is the rate of consumption of prey by an individual predator, κ is the half-saturation constant and β is the rate of conversion of prey to predator biomass. Furthermore, β/α is the conversion efficiency with the value between 0 and 1, consequently $\beta < \alpha$. The reproduction of prey is proportional to the second power of the population density specific for sexual reproduction. In the absence of predator ($\alpha = 0$) dynamics of prey is described by a bistable reaction-diffusion equation.

The coexistence (positive) equilibrium $E_*(u_*, v_*)$ of the corresponding temporal model

$$\frac{du}{dt} = au^2(b - u) - \sigma_1 u - \frac{\alpha uv}{\kappa + u} \equiv f(u, v), \tag{10}$$

$$\frac{dv}{dt} = \frac{\beta uv}{\kappa + u} - \sigma_2 v \equiv g(u, v), \tag{11}$$

is given by the equalities

$$u_* = \frac{\kappa \sigma_2}{\beta - \sigma_2}, \quad v_* = \frac{\kappa + u_*}{\alpha}\left(au_*(b - u_*) - \sigma_1\right), \tag{12}$$

and associated feasibility conditions

$$0 < \sigma_2 < \beta, \ 0 < \sigma_1 < \frac{a\kappa\sigma_2}{\beta - \sigma_2}\left(b - \frac{\kappa\sigma_2}{\beta - \sigma_2}\right)$$

which provide the positiveness of solutions.

Here we briefly present the local asymptotic stability condition of E_* for the temporal model (10)–(11) that will be required afterwards. Linearizing the nonlinear system (10)–(11) around E_* we can find the associated eigenvalue equation

$$\lambda^2 - a_{11}\lambda - a_{12}a_{21} = 0,$$

where

$$a_{11} = f_u(u_*, v_*), \ a_{12} = f_v(u_*, v_*) < 0, \ a_{21} = g_u(u_*, v_*) > 0, \ a_{22} = g_v(u_*, v_*) = 0.$$

Two eigenvalues of the above characteristic equation have negative real parts if $a_{11} < 0$ and hence E_* is locally asymptotically stable for $a_{11} < 0$. The stationary point E_* loses its stability through the super-critical Hopf bifurcation if $a_{11} = 0$.

It is well known that the models of the form (8)–(9), that is for which $a_{22} = 0$, are unable to produce any Turing pattern as the Turing instability conditions cannot be satisfied [40]. However these type of models are capable to produce non-Turing pattern if the temporal parameter values are well inside the Hopf-bifurcation domain [6]. The spatiotemporal prey-predator models with a specialist predator and linear death rate for predator population can produce spatiotemporal chaos, wave of chaos, modulated traveling wave, wave of invasion and their combinations if the spatial domain is large enough [7].

2.2. Nonlocal Model

Under the assumption that prey can move from one location to another one to access the resources, model (8)–(9) can be extended to the model with nonlocal consumption of resources:

$$\frac{\partial u}{\partial t} = d_1\frac{\partial^2 u}{\partial x^2} + au^2(b - J(u)) - \sigma_1 u - \frac{\alpha uv}{\kappa + u}, \tag{13}$$

$$\frac{\partial v}{\partial t} = d_2\frac{\partial^2 v}{\partial x^2} + \frac{\beta uv}{\kappa + u} - \sigma_2 v, \tag{14}$$

subjected to a non-negative initial condition and the periodic boundary condition. Here

$$J(u) = \int_{-\infty}^{\infty} \phi(x-y)u(y,t)dy, \quad \phi(y) = \begin{cases} \frac{1}{2M} & , \quad |y| \le M \\ 0 & , \quad |y| > M \end{cases}.$$

Various forms of kernel functions are considered in literature. Here we consider the step function for simplicity of mathematical calculations [49]. This step function means that the nonlocal consumption is confined within the range $2M$, and the efficacy of consumption inside this range is constant.

We will analyze stability of the homogeneous steady-state (u_*, v_*). We consider the perturbation around it in the form

$$u(x,t) = u_* + \epsilon_1 e^{\lambda t + ikx}, \quad v(x,t) = v_* + \epsilon_2 e^{\lambda t + ikx}, \quad |\epsilon_1|, |\epsilon_2| \ll 1.$$

The characteristic equation writes as $|H - \lambda I| = 0$ where

$$H = \begin{bmatrix} a_1 - au_*^2 \frac{\sin kM}{kM} - d_1 k^2 & -a_2 \\ b_1 & -d_2 k^2 \end{bmatrix} \tag{15}$$

and

$$a_1 = abu_* - au_*^2 + \frac{\alpha u_* v_*}{(\kappa + u_*)^2}, \quad a_2 = \frac{\alpha u_*}{\kappa + u_*}, \quad b_1 = \frac{\beta u_* v_*}{(\kappa + u_*)^2}. \tag{16}$$

Therefore, the characteristic equation becomes as follows:

$$\lambda^2 - \Gamma(k,M)\lambda + \Delta(k,M) = 0, \tag{17}$$

where

$$\Gamma(k,M) = a_1 - au_*^2 \frac{\sin kM}{kM} - (d_1 + d_2)k^2, \tag{18}$$

$$\Delta(k,M) = \left(au_*^2 \frac{\sin kM}{kM} - a_1 + d_1 k^2 \right) d_2 k^2 + a_2 b_1. \tag{19}$$

The homogeneous steady-state is stable under space dependent perturbations if the following two conditions are satisfied:

$$\Gamma(k,M) < 0, \quad \Delta(k,M) > 0 \tag{20}$$

for all positive real k and M. The homogeneous steady-state loses its stability through the spatial Hopf bifurcation if $\Gamma(k_H, M) = 0, \Delta(k_H, M) > 0$ for some k_H, and through the Turing bifurcation if $\Gamma(k_T, M) < 0, \Delta(k_T, M) = 0$ for some k_T.

2.3. Spatial Hopf Bifurcation

First, we find the spatial Hopf bifurcation threshold in terms of the parameter d_2. It is important to note that $\Gamma(k,M) < 0$ and $\Delta(k,M) > 0$ as $M \to 0+$ if we assume that (u_*, v_*) is locally asymptotically stable for the temporal model (10)–(11). One can easily verify that $\lim_{M\to 0+} \Gamma(k,M) = a_{11}$ and $\lim_{M\to 0+} \Delta(k,M) = -a_{12}a_{21}$. For some suitable M if one can find a unique value $k \equiv k_H$ such that $\Gamma(k,M) = 0$ then k_H is the critical wavenumber for the spatial Hopf bifurcation. This critical wavenumber can be obtained by solving the following two equations simultaneously:

$$\Gamma(k,M) = 0, \quad \frac{\partial}{\partial k}\Gamma(k,M) = 0. \tag{21}$$

Using the expression of $\Gamma(k, M)$, we find d_2 from the equation $\Gamma(k, M) = 0$:

$$d_2(k) = \frac{1}{k^2} \left[a_1 - a u_*^2 \frac{\sin kM}{kM} - d_1 k^2 \right]. \tag{22}$$

Substituting this expression into the second equation in (21) we get:

$$2a_1 + a u_*^2 \cos kM - 3 a u_*^2 \frac{\sin kM}{kM} = 0. \tag{23}$$

Equation (23) can have more than one positive real root depending upon the values of parameters. It is necessary to verify that the corresponding values of $d_2(k)$ are positive. We choose the root k_H for which $d_2(k_H)$ is the minimal positive number, and $\Delta(k_H, M) > 0$.

Consider, as example, the following values of parameters:

$$a = 1, \ b = 1, \ \sigma_1 = 0.1, \ \alpha = 0.335, \ \kappa = 0.4, \ \beta = 0.335, \ \sigma_2 = 0.2, \ d_1 = 1. \tag{24}$$

Then $u_* = 0.593$, $v_* = 0.419$, and Equation (23) possesses only one positive root $k = 0.297$ for $M = 6$. From (22), we find $d_2 = 0.51$. Since $\Delta(0.51, 6) = 0.0094$, these values of k and d_2 correspond to the desired spatial Hopf bifurcation thresholds, $k_H = 0.297$, $d_{2H} = 0.51$.

Furthermore, $\Gamma(k, 6) > 0$ for $d_2 < d_{2H}$. Hence the spatial Hopf bifurcation takes place as d_2 crosses the critical threshold d_{2H} from higher to lower values. Therefore, oscillatory in space and time patterns emerging due to the spatial Hopf bifurcation are observed below the stability boundary. The spatial Hopf bifurcation curve in the (M, d_2)-parameter space is shown in Figure 1. Spatiotemporal patterns for parameter values lying in the spatial Hopf domain is presented in Figure 3a.
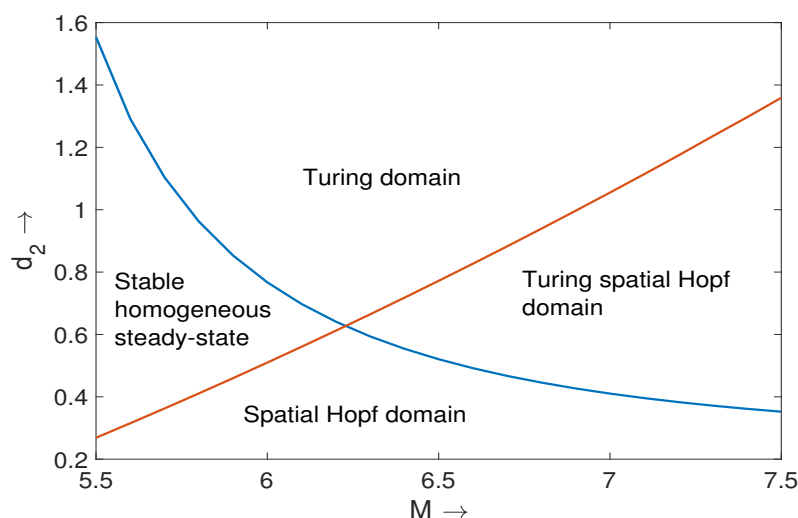

Figure 1. Turing and Hopf stability boundaries in the (M, d_2)-parameter plane.

2.4. Turing Pattern for Nonlocal Prey-Predator Model

Next, we discuss the Turing bifurcation condition and we assume that $\lim_{M \to 0+} \Gamma(k, M) < 0$ and $\lim_{M \to 0+} \Delta(k, M) > 0$. These conditions provide stability of the homogeneous steady-state under space independent perturbations. The critical wavenumber and the corresponding Turing bifurcation threshold in terms of d_2 can be obtained as a solution of the following two equations:

$$\Delta(k, M) = 0, \ \frac{\partial}{\partial k} \Delta(k, M) = 0. \tag{25}$$

From $\Delta(k, M) = 0$, we get

$$d_2(k) = \frac{a_2 b_1}{k^2 \left[a_1 - d_1 k^2 - a u_*^2 \frac{\sin kM}{kM} \right]}. \tag{26}$$

Substituting this expression into the second equation in (25), we obtain

$$4 d_1 k^2 - 2 a_1 + a u_*^2 \left(\cos kM + \frac{\sin kM}{kM} \right) = 0. \tag{27}$$

This equation can have more than one positive root. From now on, we assume that all parameter values are fixed except for M and d_2. Suppose that for a chosen value of M, (27) admits a finite number of positive roots, $k_1, k_2, \cdots, k_m$. The corresponding values of $d_2(k_i)$ in (26) are not necessarily positive. The Turing bifurcation threshold d_{2T} is given by the minimal positive value $d_2(k_i)$, and k_T is the value of k_i for which the minimum is reached.

Let us consider the same set of parameters as in the previous subsection except for $d_1 = 0.4$. An interesting feature of the Turing bifurcation curve is that it is not smooth when plotted in the (M, d_2)-parameter plane (Figure 2). The point of non-differentiability arises around $M = 12.65$. For $M = 12.5$, we find four positive roots of (27), $k_1 = 0.038$, $k_2 = 0.470$, $k_3 = 0.638$ and $k_4 = 0.786$. The corresponding values $d_2(k_{j_r})$ are positive for the last three roots, $d_2(k_2) = 0.198$, $d_2(k_3) = 0.235$ and $d_2(k_4) = 0.199$. Hence we find the Turing bifurcation threshold $d_{2T} = 0.198$, corresponding to k_2 (Figure 2b). Next, if we choose $M = 12.7$, then we find $k_1 = 0.0378$, $k_2 = 0.465$, $k_3 = 0.620$, $k_4 = 0.781$, and $d_2(k_2) = 0.201$, $d_2(k_3) = 0.232$, $d_2(k_4) = 0.189$ are positive d_2-values. Hence, the Turing bifurcation threshold $d_{2T} = 0.189$ corresponds to k_4 (Figure 2c). Hence, the point where the stability boundary is not smooth correspond to the sudden change of the location of the feasible root of Equation (27).
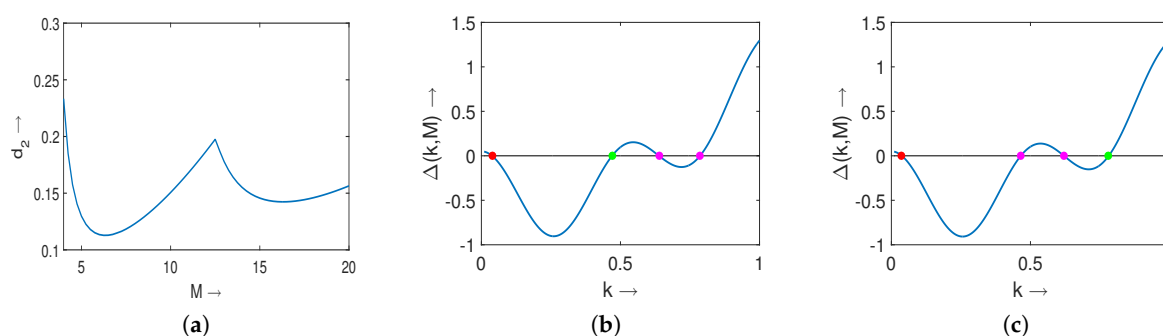

Figure 2. Turing bifurcation curve on the (M, d_2)-parameter plane (**a**). Stationary Turing patterns exist above the bifurcation curve. The functions $\Delta(k, 12.5)$ (**b**) and $\Delta(k, 12.7)$ (**c**). The root corresponding to the Turing instability is shown in green.

Finally, it is important to mention that the choice of parameters (24) leads to an interesting scenario for which the spatial Hopf and Turing bifurcation curves intersect. The two curves are shown in Figure 1 for $d_1 = 1$, and they divide the parametric domain into four different regions. Spatial patterns produced by the prey population for parameter values taken from spatial Hopf domain and Turing domain are presented in Figure 3a,b. In order to emphasize the fact that the stationary Turing pattern can be obtained for equal diffusion coefficients, we set $d_1 = d_2 = 1$ and observe a periodic in space and stationary in time solution (see Figure 3b). Various spatio-temporal patterns are observed for the values of parameters at the intersection of Turing and Hopf instability regions. Some of them are described in Section 3.
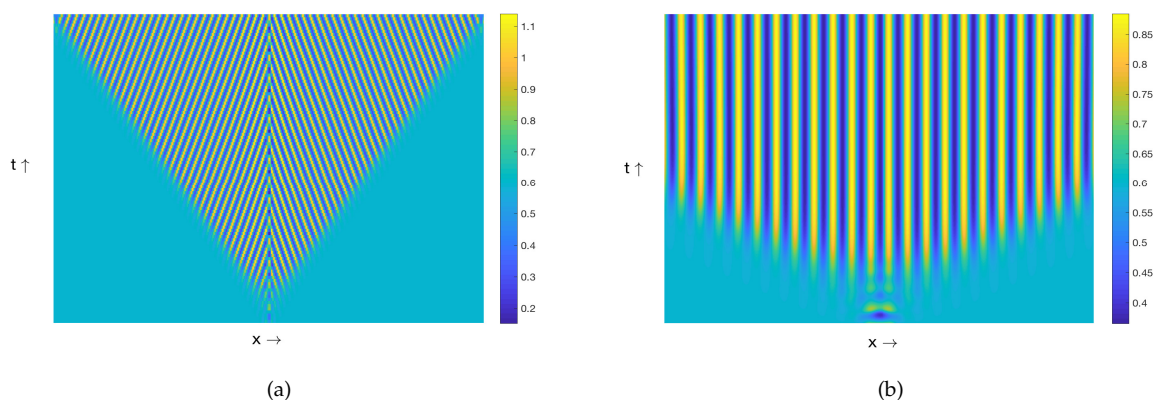
(a)　　　　　　　　　　　　　　　　　　　　(b)

Figure 3. (**a**) Resulting spatio-temporal patterns produced by the nonlocal model (13)–(14) for $d_2 = 0.3$, $M = 6.5$ and other parameter values as mentioned in the text. (**b**) Stationary pattern produced by the prey population for $d_1 = 1$, $d_2 = 1$ and $M = 6$, other parameters are mentioned at text.

3. Spatiotemporal Patterns

In this section, we study nonlinear dynamics of the prey-predator model without and with nonlocal term in the equation for prey population. We present the results of numerical simulations performed with a finite difference approximation of systems (8)–(9) and (13)–(14).

3.1. Patterns Produced by the Model (8)–(9)

In this subsection, we consider the non-Turing patterns described by system (8)–(9) in the interval $-L \leq x \leq L$ with non-negative initial condition and periodic boundary condition. Results presented here are obtained for $L = 200$. We consider a small perturbation around the homogeneous steady-state at the center of the domain as initial condition. The values of parameters are as follows

$$a = 1, b = 1, \sigma_1 = 0.1, \alpha = 0.4, \kappa = 0.4, \sigma_2 = 0.2, d_1 = 1, d_2 = 1, \tag{1}$$

and the value of β will vary.

It is known [6,7,16,26,50] that the prey-predator models with specialist predator can manifest time dependent spatial patterns if the parameters of the reaction kinetics are far inside the temporal Hopf domain. In this case, the temporal Hopf-bifurcation threshold is $\beta_* = 0.339$, that is E_* is stable for $\beta < \beta_*$, and it is unstable otherwise.

Solutions homogeneous in space and oscillatory in time are observed for $\beta > \beta_*$ but close to it. The spatiotemporal pattern presented in Figure 4a is almost homogeneous in space but oscillatory in time for the value of β close to the temporal Hopf bifurcation threshold. For larger values of β we find spatiotemporal patterns periodic both in space and time (Figure 4b) and symmetric around $x = 0$. This symmetry is maintained due to the choice of symmetric initial condition. With the increase of β we observe various complex aperiodic spatiotemporal regimes (Figure 4c). They are characterized by specific triangular patterns resulting from the merging of two peaks in the population density moving towards each other.

This model is capable to produce other type of spatiotemporal patterns, such as the traveling wave, periodic travelling wave, wave of invasion, wave of chaos similar to the prey-predator model with Rosenzweig-MacArthur reaction kinetics [26] but those results are beyond the scope of this work and will be addressed in the future.
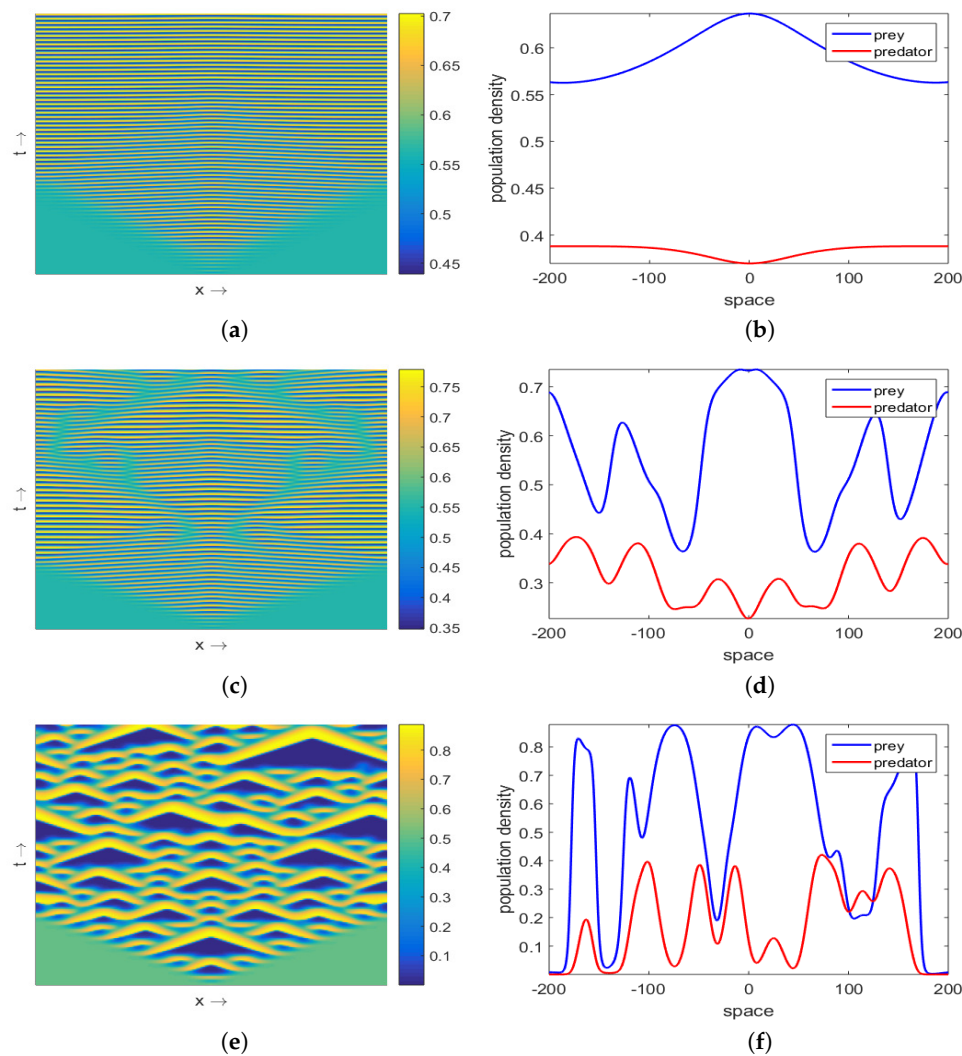
Figure 4. Spatiotemporal patterns (prey density) produced by the model (8)–(9) are presented in the left column for the parameter values as mentioned at the text and (**a**) $\beta = 0.342$; (**c**) $\beta = 0.3445$; (**e**) $\beta = 0.36$. Corresponding distribution of prey and predator population over space at $t = 1000$ are presented in the right column, see (**b**), (**d**), (**f**).

3.2. Effect of Nonlocal Consumption

We will now analyze how the nonlocal term influences dynamics of the prey-predator model. Nonlinear dynamics of prey-predator system with nonlocal consumption of resources by prey is summarized in the diagram in Figure 5a. Parameter regions with different regimes are shown on the (M, β)-plane for the values of other parameters given in (1). For small β, predator disappears while the population of prey is either homogeneous in space or it forms a spatially periodic distribution. For large β, both population go to extinction. More interesting behavior is observed for the intermediate values of β. This can be homogeneous or inhomogeneous in space, stationary or non-stationary in time solutions. Some of the spatiotemporal patterns are shown in Figure 6. For M sufficiently small these patterns become similar to those presented in Figure 4. For M large enough, both prey and predator densities represent stationary periodic in space distributions (similar to Figure 3b). Figure 5b shows a similar diagram in the case of different diffusion coefficients of prey and predator, $d_1 = 0.7, d_2 = 0.5$, with the same values of other parameters. The region of spatiotemporal patterns exists here for a narrower interval of β while the regions of stationary patterns and of extinction change their shape.
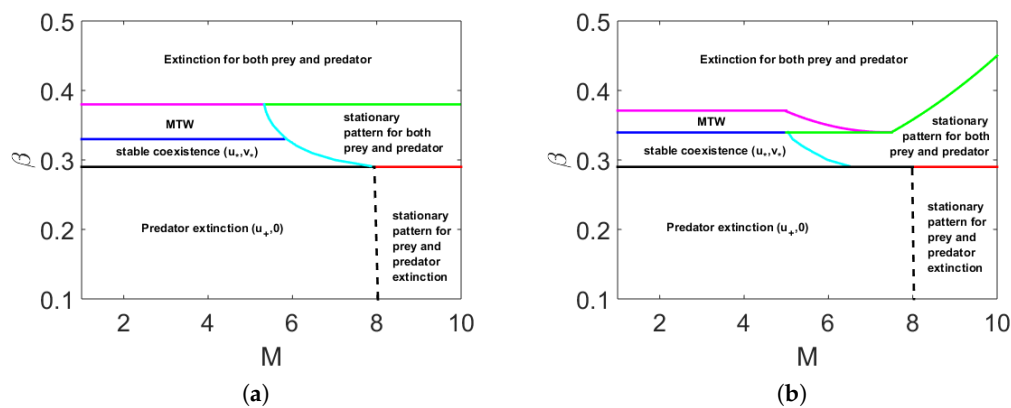
(a)　　　　　　　　　　　　　　　　　　　　　　　(b)

Figure 5. Bifurcation diagram in (M, β)-parameter space for fixed parameters $a = 1, b = 1, \sigma_1 = 0.1$, $\alpha = 0.4, \kappa = 0.4$ and $\sigma_2 = 0.2$. (**a**) $d_1 = 1, d_2 = 1$; (**b**) $d_1 = 0.7, d_2 = 0.5$.
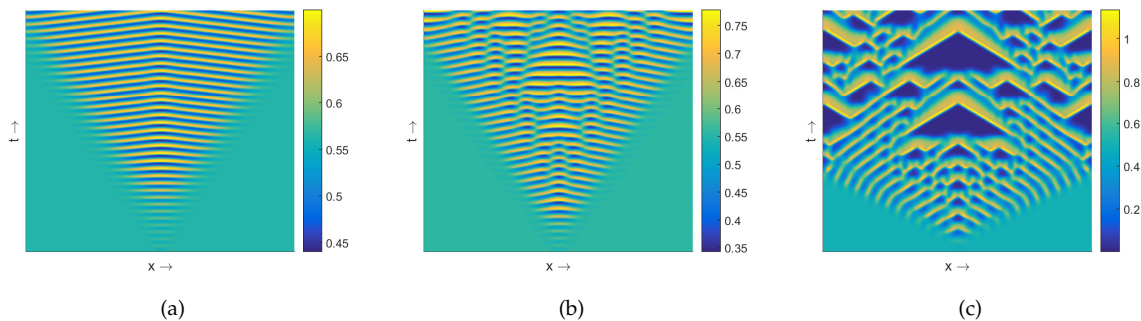

(a)　　　　　　　　　　　　　　(b)　　　　　　　　　　　　　　(c)

Figure 6. Spatio-temporal patterns produced by the nonlocal model with parameter values as mentioned at (1) with $\beta = 0.342$ and (**a**) $M = 0$; (**b**) $M = 4$; (**c**) $M = 6$.

Multiplicity of Stationary Solutions

Another interesting aspect of the stationary patterns arising through the Turing bifurcation for the spatiotemporal model with nonlocal interaction term is the existence of multiple stationary solutions for a particular value of M. We have used forward and backward numerical continuation method to determine the range of M for the stationary patterns with different periodicity (Figure 7). Fixed parameter values are same as (1) except $d_1 = 0.4$ and $d_2 = 0.2$. For example, stationary pattern with 33 patches (over a spatial domain of size $L = 200$) exists for $2 \leq M \leq 4.5$, with 32 patches for $2.5 \leq M \leq 5$, and so on.
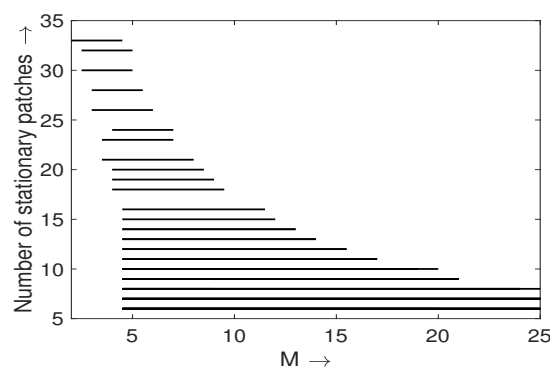

Figure 7. Stationary patterns with various number of patches exist for a range of nonlocal consumption (M) is plotted. Parameter values are same as in (24) except $d_1 = 0.4$ and $d_2 = 0.2$.

4. Discussion

In this work we study a prey-predator model with a bistable nonlocal dynamics of prey. Without the interaction with predator, the prey density is described by a bistable reaction-diffusion equation taking into account the Allee effect or the sexual reproduction of population. In this case, the reproduction rate is proportional to the second power of the population density. The dynamics of the prey population changes due to introduction of nonlocal consumption of resources. The main difference compared to the results of conventional local consumption is that the positive stable equilibrium may become unstable resulting in the appearance of stationary in time but periodic in space solutions.

The interaction with predator provides an additional factor that influences the dynamics of solutions. If we characterize this interaction by the parameter β, which determines the reproduction rate in the equation of predator density, then we can identify three main types of behavior depending on its value (Figure 5). If it is sufficiently small then the predator population vanishes since the reproduction is not enough to overcome the mortality. If this parameter is too large, then both populations go to extinction, particularly due to the bistability of the prey dynamics. Both populations coexist in a relatively narrow interval of the interconnection parameter. There are three different types of patterns inside this parameter domain. The homogeneous in space equilibrium can be stable or it can lose its stability resulting in the emergence of spatiotemporal patterns. They are observed for limited values of the parameter M which determines the range of nonlocal consumption. If the range of nonlocal consumption is sufficiently large, then both populations represent a periodic in space distribution. Such solutions are specific for nonlocal consumption with a large range, in particular for the single prey population. Thus, nonlocal consumption takes over spatiotemporal oscillations specific for the local prey-predator dynamics. Let us note that there is multiplicity of stationary patterns for the same values of parameters. This effect is specific for the problems with nonlocal interaction [39].

Spatiotemporal oscillations are specific for the prey-predator dynamics [6,7,16,26,40,50]. Here we observe the dynamics with "triangular" patterns (Figure 4) appearing when two pulses move towards each other and merge. Nonlocal consumption of resources modifies these patterns.

Some questions related to the prey-predator dynamics with nonlocal bistable model for prey remain beyond the scope of this work. We have not discussed here travelling waves and pulses that can also be observed in such models. We will study them in the subsequent work.

Author Contributions: M.B. and V.V. proposed the formulation of the problem; N.M. performed the numerical simulations; M.B. and N.M. analyzed the results; all authors participated in the preparation of the manuscript.

References

1.   Dunbar, S.R. Travelling wave solutions of diffusive Lotka-Volterra equations. *J. Math. Biol.* **1983**, *17*, 11–32.
2.   Dunbar, S.R. Travelling waves in diffusive predator-prey equations: Periodic orbits and point-to-periodic heteroclinic orbits. *SIAM J. Appl. Math.* **1986**, *46*, 1057–1078.
3.   Sherratt, J.A. Periodic travelling waves in cyclic predator-prey systems. *Ecol. Lett.* **2001**, *4*, 30–37.
4.   Sherratt, J.A.; Smith, M. Periodic travelling waves in cyclic populations: Field studies and reaction diffusion models. *J. R. Soc. Interface* **2008**, *5*, 483–505.
5.   Volpert, V.; Petrovskii, S.V. Reaction-diffusion waves in biology. *Phys. Life Rev.* **2009**, *6*, 267–310.
6.   Petrovskii, S.V.; Malchow, H. A minimal model of pattern formation in a prey-predator system. *Math. Comp. Model.* **1999**, *29*, 49–63.
7.   Petrovskii, S.V.; Malchow, H. Wave of chaos: New mechanism of pattern formation in spatio-temporal population dynamics. *Theor. Pop. Biol.* **2001**, *59*, 157–174.
8.   Gause, G.F. *The Struggle for Existence*; Williams and Wilkins: Baltimore, MD, USA, 1935.
9.   Luckinbill, L.L. Coexistence in laboratory populations of *Paramecium aurelia* and its predator *Didinium nasutum*. *Ecology* **1973**, *54*, 1320–1327.

10. Luckinbill, L.L. The effects of space and enrichment on a predator-prey system. *Ecology* **1974**, *55*, 1142–1147.
11. Fasani, S.; Rinaldi, S. Factors promoting or inhibiting Turing instability in spatially extended prey-predator systems. *Ecol. Model.* **2011**, *222*, 3449–3452.
12. Huisman, J.; Weissing, F.J. Biodiversity of plankton by oscillations and chaos. *Nature* **1999**, *402*, 407–410.
13. Levin, S.A.; Segel, L.A. Hypothesis for origin of planktonic patchiness. *Nature* **1976**, *259*, 659.
14. Segel, L.A.; Jackson, J.L. Dissipative structure: An explanation and an ecological example. *J. Theor. Biol.* **1972**, *37*, 545–559.
15. Klausmeier, C.A. Regular and irregular patterns in semiarid vegetation. *Science* **1999**, *284*, 1826–1828.
16. Medvinsky, A.; Petrovskii, S.; Tikhonova, I.; Malchow, H.; Li, B.L. Spatiotemporal complexity of plankton and fish dynamics. *SIAM Rev.* **2002**, *44*, 311–370.
17. Shigesada, N.; Kawasaki, K. *Biological Invasions: Theory and Practice*; Oxford University Press: Oxford, UK, 1997.
18. Baurmann, M.; Gross, T.; Feudel, U. Instabilities in spatially extended predator-prey systems: Spatio-temporal patterns in the neighborhood of Turing-Hopf bifurcations. *J. Theor. Biol.* **2007**, *245*, 220–229.
19. Cantrell, R.S.; Cosner, C. *Spatial Ecology via Reaction-Diffusion Equations*; Wiley: London, UK, 2003.
20. Murray, J.D. *Mathematical Biology II*; Springer: Berlin/Heidelberg, Germany, 2002.
21. Okubo, A.; Levin, S. *Diffusion and Ecological Problems: Modern Perspectives*; Springer: Berlin/Heidelberg, Germany, 2001.
22. Banerjee, M.; Banerjee, S. Turing instabilities and spatio-temporal chaos in ratio-dependent Holling-Tanner model. *Math. Biosci.* **2012**, *236*, 64–76.
23. Banerjee, M.; Petrovskii, S. Self-organized spatial patterns and chaos in a ratio-dependent predator-prey system. *Theor. Ecol.* **2011**, *4*, 37–53.
24. Gourley, S.A.; Britton, N.F. A predator-prey reaction-diffusion system with nonlocal effects. *J. Math. Biol.* **1996**, *34*, 297–333.
25. Gourley, S.A.; Ruan, S. Convergence and travelling fronts in functional differential equations with nonlocal terms: A competition model. *SIAM J. Appl. Math.* **2003**, *35*, 806–822.
26. Sherratt, J.A.; Eagan, B.T.; Lewis, M.A. Oscillations and chaos behind predator-prey invasion: Mathematical artifact or ecological reality? *Phils. Trans. R. Soc. Lond. B* **1997**, *352*, 21–38.
27. Bessonov, N.; Reinberg, N.; Volpert, V. Mathematics of Darwin's diagram. *Math. Model. Nat. Phenom.* **2014**, *9*, 5–25.
28. Genieys, S.; Bessonov, N.; Volpert, V. Mathematical model of evolutionary branching. *Math. Comp. Model.* **2009**, *49*, 2109–2115.
29. Genieys, S.; Volpert, V.; Auger, P. Pattern and waves for a model in population dynamics with nonlocal consumption of resources. *Math. Model. Nat. Phenom.* **2006**, *1*, 63–80.
30. Genieys, S.; Volpert, V.; Auger, P. Adaptive dynamics: Modelling Darwin's divergence principle. *Comp. Ren. Biol.* **2006**, *329*, 876–879.
31. Volpert, V. Branching and aggregation in self-reproducing systems. *ESAIM Proc. Surv.* **2014**, *47*, 116–129.
32. Apreutesei, N.; Bessonov, N.; Volpert, V.; Vougalter, V. Spatial structures and generalized travelling waves for an integro-differential equation. *DCDS B* **2010**, *13*, 537–557.
33. Aydogmus, O. Patterns and transitions to instability in an intraspecific competition model with nonlocal diffusion and interaction. *Math. Model. Nat. Phenom.* **2015**, *10*, 17–19.
34. Volpert, V. Pulses and waves for a bistable nonlocal reaction-diffusion equation. *Appl. Math. Lett.* **2015**, *44*, 21–25.
35. Volpert, V. *Elliptic Partial Differential Equations*; Reaction-diffusion equations; Birkhäuser: Basel, Switzerland, 2014; Volume 2.
36. Apreutesei, N.; Ducrot, A.; Volpert, V. Competition of species with intra-specific competition. *Math. Model. Nat. Phenom.* **2008**, *3*, 1–27.
37. Apreutesei, N.; Ducrot, A.; Volpert, V. Travelling waves for integro-differential equations in population dynamics. *DCDS B* **2009**, *11*, 541–561.
38. Bayliss, A.; Volpert, V.A. Patterns for competing populations with species specific nonlocal coupling. *Math. Model. Nat. Phenom.* **2015**, *10*, 30–47.
39. Banerjee, M.; Volpert, V. Prey-predator model with a nonlocal consumption of prey. *Chaos* **2016**, *26*, 083120.

40. Banerjee, M.; Volpert, V. Spatio-temporal pattern formation in Rosenzweig-McArthur model: Effect of nonlocal interactions. *Ecol. Complex.* **2016**, *30*, 2–10.

41. Amarasekare, P. Interactions between local dynamics and dispersal: Insights from single species models. *Theor. Popul. Biol.* **1998**, *53*, 44–59.

42. Amarasekare, P. Allee effects in metapopulation dynamics. *Am. Nat.* **1998**, *152*, 298–302.

43. Courchamp, F.; Berec, L.; Gascoigne, J. *Allee Effects in Ecology and Conservation*; Oxford University Press: Oxford, UK, 2008.

44. Courchamp, F.; Clutton-Brock, T.; Grenfell, B. Inverse density dependence and the Allee effect. *Trends. Ecol. Evol.* **1999**, *14*, 405–410.

45. Lewis, M.A.; Kareiva, P. Allee dynamics and the spread of invading organisms. *Theor. Popul. Biol.* **1993**, *43*, 141–158.

46. Jankovic, M.; Petrovskii, S. Are time delays always destabilizing? Revisiting the role of time delays and the Allee effect. *Theor. Ecol.* **2014**, *7*, 335–349.

47. Petrovskii, S.; Blackshaw, R.; Li, B.L. Consequences of the Allee effect and intraspecific competition on population persistence under adverse environmental conditions. *Bull. Math. Biol.* **2008**, *70*, 412–437.

48. Banerjee, M.; Vougalter, V.; Volpert, V. Doubly nonlocal reaction diffusion equations and the emergence of species. *Appl. Math. Model.* **2017**, *42*, 591–599.

49. Segal, B.L.; Volpert, V.A.; Bayliss, A. Pattern formation in a model of competing populations with nonlocal interactions. *Physics D* **2013**, *253*, 12 – 23.

50. Petrovskii, S.V.; Li, B.L.; Malchow, H. Quantification of the spatial aspect of chaotic dynamics in biological and chemical systems. *Bull. Math. Biol.* **2003**, *65*, 425–446.